Journal of Biomechanics 48 (2015) 2034–2040

Contents lists available at ScienceDirect

Journal of Biomechanics

journal homepage: www.elsevier.com/locate/jbiomech
www.JBiomech.com

Developing CT based computational models of pediatric femurs

Xinshan Li [a,e,*], Marco Viceconti [a,e], Marta C. Cohen [b,e], Gwendolen C. Reilly [c,e], Matt J. Carré [a,e], Amaka C. Offiah [d,e]

[a] Department of Mechanical Engineering, University of Sheffield, Sheffield, UK
[b] Department of Histopathology, Sheffield Children's Hospital, Western Bank, Sheffield, UK
[c] Department of Materials Science and Engineering, University of Sheffield, Sheffield, UK
[d] Academic Unit of Child Health, University of Sheffield, Sheffield, UK
[e] Insigneo Institute for in Silico Medicine, University of Sheffield, Sheffield, UK

ARTICLE INFO

Article history:
Accepted 24 March 2015

Keywords:
Pediatric long bone
Bone development
Finite element models
Bone mechanical properties

ABSTRACT

The mechanisms of fracture in infants and toddlers are not well understood. There have been very few studies on the mechanical properties of pediatric bones and their responses under fracture loading. A better understanding of fracture mechanisms in children will help elucidate both accidental and non-accidental injuries, as well as bone fragility diseases. The aim of this study is to develop *in silico* femoral models from CT scans to provide detailed quantitative information regarding the geometry and mechanical response of the femur, with the long term potential of investigating injury mechanisms. Fifteen anonymized QCT scans (aged 0–3 years) were collected and used to create personalized computational models of femurs. The elastic modulus of femur was illustrated at various ages. The models were also subjected to a series of four point bending simulations taking into account a range of loads perpendicular to the femoral shaft. The results showed that mid-shaft cross-section at birth appeared circular, but the diameter in the anteroposterior axis gradually increased with age. The density, and by implication modulus of elasticity at the mid-shaft became more differentiated with growth. Pediatric cortical bone with density close to the peak values found in adults was attained a few weeks after birth. The method is able to capture quantitative variations in geometries, material properties and mechanical responses, and has confirmed the rapid development of bone during the first few years of life using *in silico* models.

1. Introduction

Fractures in infants and young children are relatively uncommon and can be broadly categorized as following either accidental (either of normal or of abnormal bone) or abusive (also referred to as non-accidental or inflicted) mechanisms. Accidental injury usually occurs once the child begins to walk unaided. Abusive injury on the other hand, is most often seen before 2 years of age, which frequently presents a diagnostic dilemma since the child is less capable of conveying the sequence of events (Fassier et al., 2013, Pierce et al., 2004). There are currently no available tools to quantitatively examine a child's injury in relation to the physiology of the bone and the descriptions provided by the carers. Determining whether a stated mechanism could actually have caused the identified fracture(s) is not straightforward. Many parameters such as the age, height of fall, velocity at impact, impact materials and directions need to be taken into account. Biomechanical models, with their capability to test different scenarios, will ultimately help to answer these questions, but there has been little development of such models in the pediatric age group.

The morphology and biomechanics of pediatric bone is considerably different from the adult (Currey et al., 1996, Ohman et al., 2011, Vinz, 1972, 1970, 1969). The change in femoral shape over age is illustrated in Fig. 1(a). At birth, the most prominent femoral structure viewed in X-ray is its shaft. A small ossification region can also be observed, which then develops into the distal epiphysis. The proximal ossification center however, does not appear until a few months after birth. These observations correlate well with those described in Scheuer et al. (2000). Both ossification centers are linked to the shaft by cartilage, which cannot be clearly seen in X-ray or computed tomography (CT).

Mechanical data on children's bone is scarce, particularly for children younger than 3 years of age. The majority of experiments have been carried out on the cortical components of long bones (Hirsch and Evans, 1965, Vinz, 1972, 1970, 1969 Currey and Butler,

* Corresponding author at: Department of Mechanical Engineering, University of Sheffield, Sheffield, UK. Tel.: +44 114 222 7786; fax: +44 114 222 7890.
E-mail addresses: xinshan.li@sheffield.ac.uk (X. Li), m.viceconti@sheffield.ac.uk (M. Viceconti), Marta.Cohen@sch.nhs.uk (M.C. Cohen), g.reilly@sheffield.ac.uk (G.C. Reilly), m.j.carre@sheffield.ac.uk (M.J. Carré), a.offiah@sheffield.ac.uk (A.C. Offiah).

http://dx.doi.org/10.1016/j.jbiomech.2015.03.027
0021-9290/

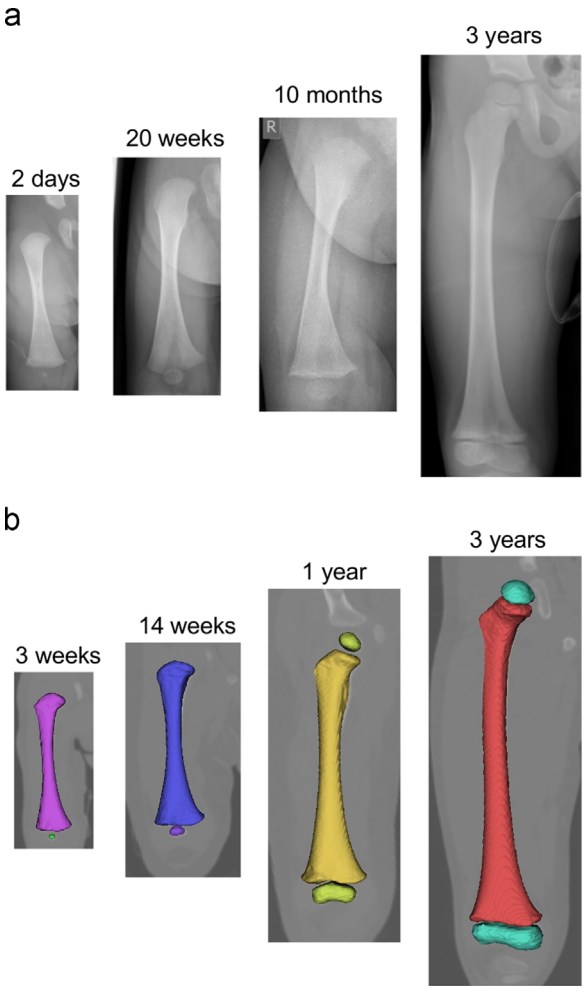

Fig. 1. (a) X-ray images of femurs for 0–3 years old (from a different cohort collected at the Sheffield Children's Hospital), showing the gradual change in length and diameter, as well as the ossification process at the epiphyses. (b) Segmented geometries of right femurs (anterior view) of children at different ages showing the diaphysis and epiphyseal ossification centers. Segmentation results overlap the original CT scans.

1975, Currey and Pond, 1989, Currey et al., 1996); most studies were conducted before 2000 with only one recent study by Ohman et al. (2011). These studies have all used isolated bone samples with the number of individuals being studied ranging from 3 to 25 cases, compared with 15 cases in this study. It should be noted that the statistical power is limited here due to the small number of cases. This is partly due to the scarcity of pediatric data. As an on-going clinical study, we plan to add more cases in the cohort in the near future. Table 1 summarizes these previous studies. Currey et al. (1996) carried out a series of fracture (proximal femurs) and impact (distal femurs) experiments using specimens between 4 and 82 years old, and found that the age and ash density were highly correlated ($R^2=74\%$). This is in agreement with the recent study conducted by Ohman et al. (2011), which showed strong correlation between ash density and compressive elastic (or Young's) modulus ($R^2=86$–91%) (4 to 15 years old). The study suggested that the methods developed for modeling adult bones could be tailored to pediatric applications. Furthermore, Ohman's paper has also highlighted the rarity of pediatric bone samples with only 12 child patients being reported aged 4 to 15 years old.

Only one study has reported on the compressive behavior of trabecular bone in the femur of children (McCalden et al., 1997). The authors suggest that the strong relationship between strength and apparent density of cancellous bone supports the use of non-invasive methods (e.g. CT) to estimate bone density in order to predict changes in bone strength (McCalden et al., 1997). Therefore the approach used to derive the Young's modulus of adult bone from measured CT Hounsfield Units will be applied here to the modeling of children's bone (Taddei et al., 2003, 2007, Schileo et al., 2008a).

This study focuses on investigating the biophysics of the right femur in very young children between 0 and 3 years old. By adopting an *in silico* approach of engineering biomechanics, the aims of this study are to: (a) apply a well-established approach for adult femurs to very young children by creating 3D personalized virtual femurs using quantitative computed tomography (QCT) images; (b) accurately capture the geometry and mechanical properties of pediatric femurs; (c) derive quantitative morphological data (diameters, lengths, modulus of elasticity) to elucidate the changes in the growing bone and (d) perform preliminary analysis on the predicted mechanical response of developing femurs under four point bending.

2. Materials and methods

This study involved retrospective investigation of anonymized QCT images obtained as part of a local post mortem examination at the Sheffield Children's Hospital. Local policy is that blanket informed consent for research is obtained from parents or legal guardians at the time of obtaining consent for the post-mortem, with the option to withhold consent for the use of images. Local Research Ethics Committee approval was waived on the understanding that consented parents or legal guardians had not opted out of images or data being used for research. The study was registered with our local Research & Development Department (study registration number CA11024). The local policy also applies to the X-ray images shown in Fig. 1(a), obtained at the same hospital from a different cohort.

Fifteen sets of whole body QCT scans were collected as part of an on-going project to investigate the use of CT in post-mortem examinations, particularly for cases of sudden infant death syndrome (SIDS), sudden unexpected death in infancy (SUDI) and childhood (SUDC). There is no observable pathology reported in the histology analysis that would affect the normal development of bone. The CT images were obtained using a GE Lightspeed 64-slice CT scanner, with an image resolution of $0.625\times0.625\times0.625\ mm^3$. The data was anonymized for the purposes of this study. The age for each individual was corrected for prematurity at birth (40 weeks as full term). The height was measured from the crown of the head to the toe. Percentiles for weight and height were obtained from the Child Growth Foundation Tables (for Boys and Girls, http://childgrowthfoundation.org).

Based on the CT scans, personalized computational models of pediatric femurs were created using a well-established approach for adult femurs (Schileo et al., 2008a, 2008b). This approach has been well validated (in adults) against in vitro experiments to investigate fracture mechanisms in the femur under various loading conditions (Schileo et al., 2007, Grassi et al., 2012, Cristofolini et al., 2010). The following sections provide a detailed description of our application of this method to create femoral models in very young children.

2.1. Mesh generation

The CT scans were segmented using ITK-snap (ITK, http://www.itksnap.org) in order to obtain the femoral outlines. Because cartilage in the growth region cannot be differentiated from surrounding soft tissues, only the ossified bones were considered during this segmentation process. A threshold value of 350 Hounsfield Units was used to select pixels representing ossified bone. This value was chosen to ensure reliable detection at the edge of the diaphysis by accounting for boundary pixels containing both bony and soft tissues. A trained operator manually checked all segmentation results by overlapping the segmented geometry with the original CT scans. Fig. 1(b) shows the segmented geometries from children at the age of 3 weeks, 14 weeks, 1 year, and 3 years.

For each individual, the length of the femur was estimated by calculating the distance between the proximal and the distal ossification centers. The distal ossification center was relatively straightforward to estimate because it was present at birth, while the proximal ossification center did not appear until a few months later. In these cases, the proximal ossification center was approximated using the bony boundaries of the proximal femur and the acetabulum as illustrated in Fig. 2.

2.2. Young's modulus estimation

The CT scans were calibrated using the European Spine Phantom (ESP). Using a well-established approach for estimating adult bone material properties from CT scans (Schileo et al., 2008a, 2008b; Zannoni et al., 1998, Taddei et al., 2004), a linear

Table 1
Previous literature on cortical bone mechanical properties of children.

Author	Age (yrs)	Number of specimen	Specimen shape	Origin	Mechanical test	Young's modulus (GPa)
Hirsch and Evans (1965)	0–14	16	Rectangular	Femur	Tension	7–33
Weaver (1966)	2–87	–	Rectangular	Fibula, tibia, ulna, ilium	Indentation	–
Vinz (1969, 1970, 1972)	0–85	198	–	Femur	Tension	10–33 (< 14 yrs)
Yamada (1970)	10–79	36 subjects	–	Femur	Tension and bending	N/A
Currey and Butler (1975)	2–14	59	Rectangular	Femur (mid-shaft)	Three-point bending	3–14
Currey and Pond (1989)	3–5	3	Rectangular	Femur	Tension	7–13
Currey et al. (1996)	4–82	88	Rectangular	Femur	Three-point bending; Hounsfield plastics impact test	–
Ohman et al. (2011)	4–15	43	Cylindrical	Femur, tibia	Compression	5–15

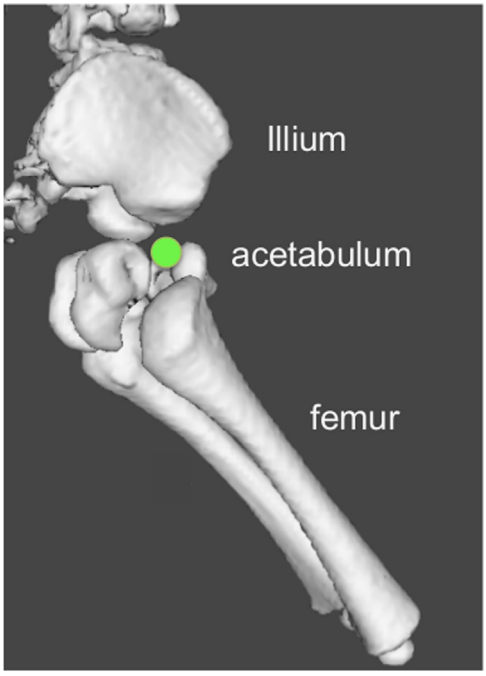

Fig. 2. Sagittal view of the thigh and hip skeleton showing the estimated center of ossification (green dot) in the proximal epiphysis, which represents the mid-point between the femur and the acetabulum. (For interpretation of the references to color in this figure legend, the reader is referred to the web version of this article.)

relationship was estimated between the grayscale value (*gray*) and the CT density (ρ_{CT}):

$$\rho_{CT} = 0.0007035\, gray - 0.01185 \quad (1)$$

The apparent density of bone (ρ_{app}) was estimated by assuming the following relationships with the ash density (ρ_{ash}), derived from adult bones (Schileo et al., 2008a):

$$\rho_{ash} = 0.8772\, \rho_{CT} + 0.07895 \quad (2)$$

$$\rho_{app} = \frac{1}{0.6}\rho_{ash} \quad (3)$$

The Young's modulus (E) was then estimated based on the following relationship proposed by Morgan et al. (2003):

$$E = 6850\rho_{app}^{1.49} = 14664\rho_{ash}^{1.49} \quad (4)$$

Finite element meshes of the femurs consisting of 10-node tetrahedra were created using ANSYS. The number of elements was adjusted to be proportional to the femoral length. The meshes were imported into the LHPBuilder where the Young's modulus was calculated as described above using BONEMAT3 (Schileo et al., 2008a). This resulted in a final finite element mesh with each element containing the averaged Young's modulus integrated from surrounding pixels in the original CT scans. Therefore, the computational femoral model contained personalized information in both geometry and material properties.

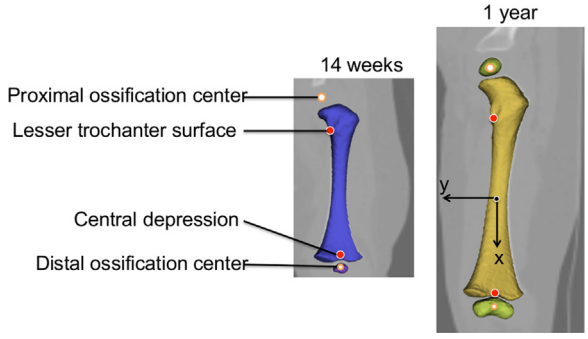

Fig. 3. The four landmarks selected for repeatability tests are illustrated in the segmented right femurs in the posterior view. The proximal ossification center in the 14 weeks old child was estimated. The resulting reference system is illustrated in the 1-year-old femur.

2.3. Reference system

The conventional coordinate system (Wu et al., 2002) used in adult femur cannot be readily applied here due to the absence of the epiphyses. Therefore, a new reference system needs to be developed based on available features of very young children's femurs. Four potential landmarks were considered in this study: the proximal and the distal ossification centers, the lesser trochanter surface, and the central depression (intercondylar notch in adult femur) (see Fig. 3). A repeatability test was carried to select the two most reliable landmarks, which are the proximal and the distal ossification centers.

To create the new reference system, the middle point between two ossification centers was defined as the origin, which approximated the location of the mid-shaft. The x direction points to the inferior from the origin to the distal ossification center (see Fig. 3). The y direction points medially to the proximal ossification center. The z direction points to the anterior perpendicular to the x–y plane.

2.4. Boundary constraints

To simulate four point bending, the femoral shaft was isolated, representing 50% of the total femoral length (see Fig. 4). The lowest nodes (in y direction) at both ends of the shaft were assumed to be the support points. Nodes at the ends of the shaft were constrained so that translations were partially permitted in x, y and z directions (see Fig. 4 for more detail). Forces of equal magnitude were applied where the loading span equaled half of the support span. The amount of force applied was estimated empirically in order for the maximum first principal strain to reach a yield value of 0.73% (assuming bone fails first in tension) (Bayraktar et al., 2004).

Starting with the default orientation where forces were applied towards the lateral direction (or negative y direction), the femur was rotated 10 degrees around the shaft (or x direction) for each subsequent simulation in order to include a range of loading orientations perpendicular to the shaft (see Fig. 4). For each orientation, the maximum first and third principal strains were evaluated at each node in the

region of interest (ROI). Due to the change in size with developing bones, convergence analysis was repeated for femurs at various ranges of lengths. The number of elements of the finite element meshes used in this study ranged between 86,000 and 160,000.

3. Results

The demographics of each individual are shown in Table 2. The range of femoral lengths is comparable with those reported in Scheuer et al. (2000). Both height and weight were within the normal range for the majority of cases, except cases 2, 10 and 11, which were considerably lower than normal ($\leq$2nd percentile for weight and $\leq$9th percentile for height).

The femoral length, and height and weight of each child were relatively well correlated. In general, the length of the femur, which varied between 7.7 cm and 22.4 cm, increased with the age. There are some slight variations in the group. A few individuals (cases 2, 10 and 11) showed slightly shorter femoral lengths than the others at a similar age. Case 2 at the age of 2 weeks had a very low body weight (2nd percentile) shown in Table 2. Case 11 at the age of 20 weeks was six weeks premature, with low values in both body weight (2nd percentile) and height (9th percentile).

Mid-shaft diameters in the anterior–posterior (AP) and medial–lateral (ML) directions are plotted in Fig. 5. Bones from individuals younger than 1 year old (cases 1 to 12) had an ML diameter similar to or greater than AP, except case 3. For those more than 1 year old (cases 13 to 15), 2 out of 3 cases (except case 14) gave AP greater than ML diameter. Distribution of the CT density and elastic (Young's) modulus in the sagittal sections of the femurs is illustrated in Fig. 6. A few weeks after birth, bone with a CT density and Young's modulus close to mature cortical bone (the more stiff bone approximately 1.1 g/cm^3 or 20 GPa) was present at the periphery of the diaphysis. As the femurs grew in length and diameter, both the density and the Young's modulus became more differentiated across the shaft.

The differential individual growth rate is illustrated in Fig. 7 using cases 3 and 11, representing advanced and delayed development, respectively. The length of the femur for case 3 (8.5 cm, 2 weeks of age) was only slightly lower than that of case 11 (9.6 cm, 16 weeks of age), despite the difference in age (see

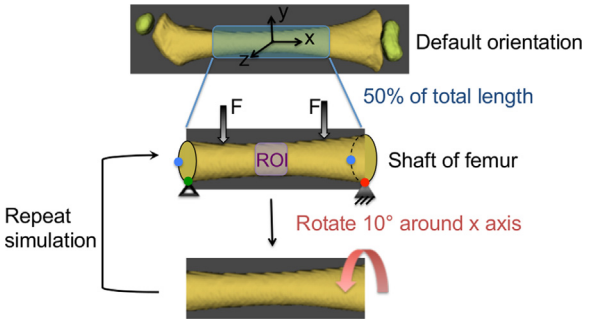

Fig. 4. Boundary constraints applied to the model and the simulation procedure for four point bending illustrated on the 1-year-old femur. ROI, region of interest. Blue nodes: fixed in *z* direction; green node: fixed in *y* direction; red node: fixed in *x*, *y* and *z* directions. (For interpretation of the references to color in this figure legend, the reader is referred to the web version of this article.)

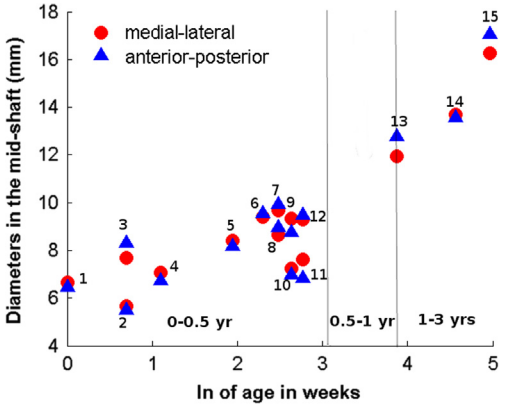

Fig. 5. Mid femoral shaft diameters plotted against ln of age. The case number is indicated beside each marker, which corresponds to information provided in Table 2.

Table 2
Demographics for the post-mortem study. The femoral length was estimated from CT scans by calculating the distance between the proximal and the distal ossification centers. The predicted failure force was the amount of force applied when the maximum first principal strain reached a yield value of 0.73% (see "Boundary constraints" section). This force was an empirical estimation with an increment of 10 N. The last column reports the ratio of the maximum first principal strains in the AP direction over the ML direction, when forces were applied directly in these directions.

Case No.	Gender	Corrected age [a](weeks)	Cause of death	Weight (g)/ percentile	Height (cm)/ percentile	Femoral lengths (cm)	Predicted failure force (N)	AP/ML max 1st PC strain
1	M	0	Pneumonia pertussis	3300/25th	51/98th	8.0	140	1.038
2	F	2	SUDI[b]	2248/2nd	47/48th	7.7	120	1.085
3	F	2	Hypoplastic left heart syndrome	4005/75th	59.5/99th	8.5	270	0.945
4	M	3	SUDI	3240/2-10th	63/50-75th	8.5	160	1.217
5	M	7	SUDI	4400/9th	55/50-75th	9.1	240	1.059
6	M	10	Severe acute bronchopneumonia	7565/99th	68/99th	10.5	350	1.065
7	F	12	SUDI	5890/50th	63/75th	10.8	300	1.23
8	F	12	SIDS[c]	6375/75th	67/ > 90th	11.1	220	1.033
9	M	14	SUDI	6505/75th	62/50th	10.6	300	1.075
10	M	14	Cardiomyopathy	4525/2nd	60/9th	9.6	160	1.22
11	M	16	SIDS	3850/ < 2nd	60/9th	9.6	160	1.214
12	F	16	SUDI	5790/ < 9th	65/91st	11.0	360	1.205
13	M	48 (1 yr)	SUDI	12980/91-99th	82.6/ > 99th	15.3	600	0.979
14	F	96 (2 yrs)	Inhalation of products of combustion	13130/75th	92/98th	18.5	670	1.074
15	F	144 (3 yrs)	Non-accidental head injury	17500/91st	102.5/98th	22.4	1040	0.957

[a] Age corrected for prematurity at birth (40 weeks as full term).
[b] SUDI, sudden unexpected death in infancy.
[c] SIDS, sudden infant death syndrome.

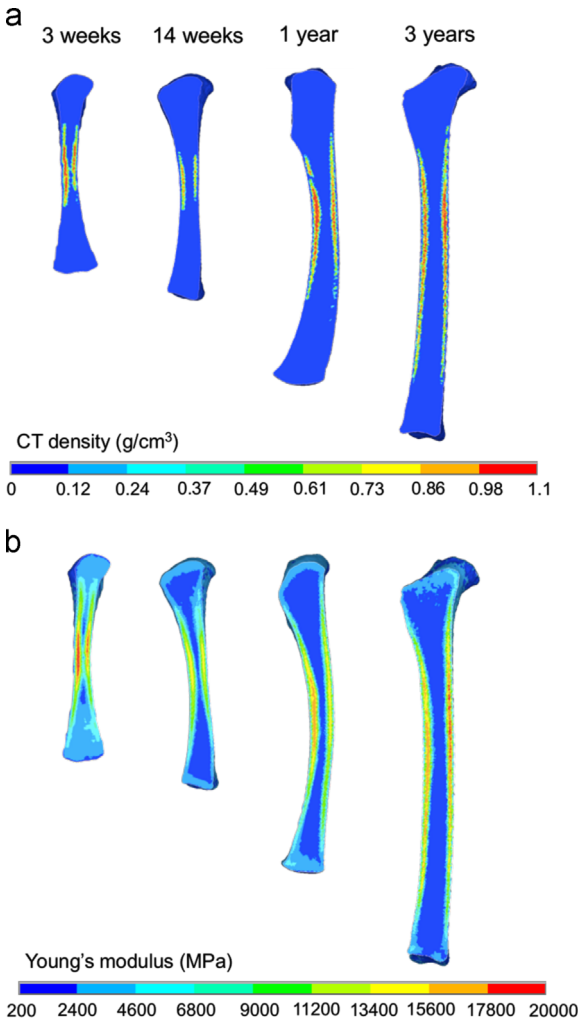

Fig. 6. CT density (a) and Young's modulus (b) estimated from the measured Hounsfield Units of CT scans at different ages. Geometries of the same individuals are illustrated in Fig. 1(b).

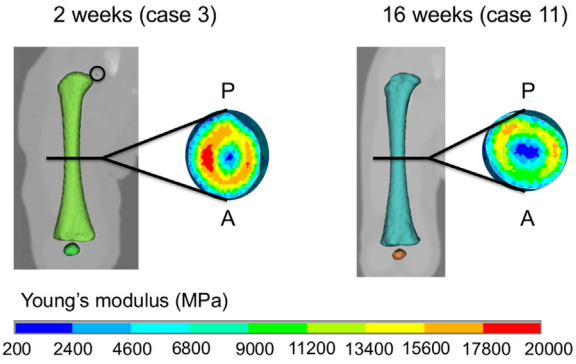

Fig. 7. Geometries and Young's modulus at the mid-shaft for 2 weeks (case 3) and 16 weeks (case 11) old children. The small but visible ossification center in the proximal epiphysis is circled in black for case 3. P, posterior; A, anterior.

Table 2). The cross-sectional dimensions at the mid-shaft were substantially different. Case 3 had a much longer AP diameter with a visible ridge (linea aspera) in the posterior aspect and increased anterior curvature, and showed signs of advanced ossification of the proximal epiphysis (black circle in Fig. 7), features that are normally observed in older children in the dataset. In contrast, although older, case 11 retained the longer diameter in the ML

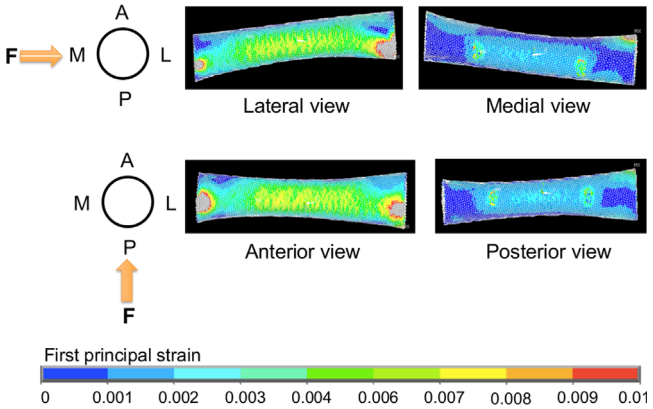

Fig. 8. First principal strain distribution of the 1-year-old femur model when force was applied towards the medial (above) and lateral (below) directions. The diagrams on the left illustrate the cross-section of the femur and the direction at which force was applied.

direction with little development of the linea aspera. According to Scheuer et al. (2000), the development of the linea aspera is very variable. However, it generally correlates with weight bearing and standing.

The amount of force predicted to "fracture" the bone (e.g. reach a maximum first principal strain of 0.73% in the ROI) ranged from 120 N to 1040 N for the 15 cases (see Table 2). These forces were estimated empirically through the finite element simulation using an increment of 10 N. The values of maximum first principal strain were also compared when forces were applied directly in the AP and ML directions. The ratio of AP over ML strain (maximum first principal strain) was reported in Table 2 for each case. For most children younger than 6 months old, the AP direction had slightly higher maximum first principal strains (approximately 4%–23% difference) than the ML direction. However, the opposite was observed for those who had a much longer AP diameter than ML diameter (cases 3, 13, and 15). The predicted mechanical responses under different bending directions are illustrated in Fig. 8 using the 1-year-old femur model.

4. Discussion

A CT-based computational modeling framework, previously used in adults, has been applied to create personalized femoral models of fifteen very young children (0–3 years of age), where new methodology was presented to set up a unique reference system according to juvenile femur anatomy and to apply appropriate boundary constraints to the bone. The models were able to capture the geometry and material properties of the developing femurs, and quantitatively demonstrate changes in morphology with age. These changes are likely to correspond to important functional adaptations during growth and development.

The analysis of geometry suggested that the mid-shaft cross-section has a more circular shape at birth. The elongation of the femoral width in the AP direction reflects the formation of the linea aspera, a ridge on the posterior aspect of the femur where numerous muscles (e.g. vastus medialis, vastus lateralis, adductor brevis, adductor longus, etc.) are attached. The change in distribution of bone density in Fig. 6 (during the first 3 years of life) reflects the development of stiff cortical bone at the periphery of the diaphysis, while the formation of the medullary (bone marrow) cavity takes place in the middle. These results suggested that normal biomechanical and anatomical differentiation of femur is interdependent.

The rate of development however, does not solely depend on age. Two outliers illustrated here were cases 3 (above average development) and 11 (below average development). Post mortem data confirmed that overall demographics (height and weight) related well to the rate of development observed in individual femurs. Both infants were of Caucasian origin and neither had started crawling at the time of death. The underlying reasons for altered development in cases 3 and 11 cannot be confirmed due to the lack of additional clinical data; however it is worth noting that case 11 was 6 weeks preterm, which may have some association with the delay in skeletal development. In addition, other factors such as physical activity and ethnicity may also play a role (Wallace et al., 2013, Cardadeiro et al., 2012, McKay and Smith, 2008). It is also common for a range of considerably different morphology and curvature to present in juvenile femurs during infancy and childhood (Scheuer et al., 2000). Therefore, the results reported here should be treated with caution, and more information is needed in order to conclusively determine if these cases are indeed outliers or part of the normal variations.

The amount of force predicted to "fracture" the femur under bending generally increased with increase in size of the femur. The AP direction appeared to be slightly weaker than the ML direction during the first 6 months, but the difference diminished after 1 year of age. One possible explanation is the elongation in the AP direction due to the development of the linea aspera. This would potentially make the bone more resistant to bending in the AP direction (Kontulainen et al., 2007). However, this effect needs to be confirmed with further studies.

Some published papers suggest a direct link between skeletal muscle function and bone adaptation. Muscle contractions place direct loads on the bone, causing it to adapt (Schoenau and Fricke, 2008, Specker, 2006, Kemper, 2000). Due to the lack of muscle information, it is difficult to investigate the relationship between the femur and muscles attached to it from this dataset. However, it can be speculated that mechanical loading is a likely factor in diameter changes at the mid-shaft as illustrated in Fig. 5, where the dominant diameter switched from the ML to AP direction between the ages of 6 and 12 months. This is the period when a baby starts to crawl, stand and toddle. This change in ambulatory pattern is expected to lead to alterations in muscle and bone function in order to adapt to the upright posture (Scheuer et al., 2000), reflected by the remarkable modification in cross-sectional geometry over a short period of time (approximately 6 months). Unfortunately in this dataset, no subject was collected within this critical window. As the post-mortem study continues with more scans being collected, further studies will be conducted to investigate the considerable change in morphology during this transitional period and its effect on the amount of force predicted to "fracture" the bone. Nevertheless, the existing data and literature strongly suggest a close relationship between bone's geometry, mechanical properties and the amount of force predicted to "fracture" the bone.

All cases reported in this study were collected as part of an ongoing investigation into the use of CT for post mortem examination of very young children (see Table 2). Some causes of death such as hypoplastic left heart syndrome in case 3 may affect the mobility of the infant and hence skeletal development. For those with sudden unexplained death in infancy, there is a possibility that underlying conditions could lead to pathological changes in the skeleton that are not visible on CT. A previous study showed that a significant proportion (76.5%) of infants and children who died suddenly had inadequate levels of Vitamin D, although only 19% had visible changes on radiology (Cohen et al., 2013). The significance of low levels of vitamin D on bone strength and fracture causation in the absence of radiological or biochemical features of rickets is debated (Arundel et al., 2012), and could potentially be determined in a future larger study using computational methods.

One limitation of this study is that the method used to estimate bone modulus of elasticity from CT scans is reliant on findings of a recent study by Ohman et al. (2011), where the author concluded that the difference in mechanical strength between pediatric and adult bone was correlated to ash density. It should be noted that the youngest child in Ohman's study was 4 years of age, which is older than the age range (0–3 years) in our dataset. Other previous literature (Currey et al., 1996) has also drawn similar conclusions as Ohman et al. (2011). However, that study was performed more than a decade ago, with less advanced technology. Therefore, more work needs to be performed in order to confirm these findings, especially for infants and toddlers.

Another limitation of the computational model is that changes in bone at the tissue level were not taken into account. These microstructural changes are influenced by the degree of mineralization, the structure of bone matrix, as well as collagen composition, which is thought to have an impact on the overall biomechanical properties (Bennett and Pierce, 2010, Mosekilde et al., 1987). For example, mature bones undergo brittle fracture (elastic deformation), while pediatric bones deform plastically, represented by a classical "greenstick fracture" (Berteau et al., 2012). This would affect the validity of the yield strain used in this study, which is based on previous experiments from adult bones (Bayraktar et al., 2004). Future studies need to be conducted at the tissue level in order to quantify these changes. One possibility is to use bones excised for histological examination and perform high-resolution peripheral QCT and indentation tests to ascertain mechanical properties. However, the availability of fresh bone samples remains the greatest hurdle for such studies.

In conclusion, this study confirmed that the structural and mechanical properties of pediatric femurs can be captured using a CT-based modeling approach. These two factors also appeared to be interdependent. Future studies will be conducted to investigate femoral fracture patterns under a variety of loading conditions using these personalized computational models. Validation studies could be carried out using animal bones subjected to four point bending tests and later on by qualitatively comparing simulation results with known fracture cases reported in the clinic. These studies will help elucidate fracture mechanisms in children by predicting failure loads under specific loading scenarios, allowing more robust verification of the mechanisms and thereby improving our ability to diagnose.

Conflict of interest

The authors have no conflict of interest to declare.

Acknowledgments

The authors would like to thank CT radiographers Rebecca Ward and Elzene Kruger for their help with imaging and data acquisition. This project was financially supported by The Children's Hospital Charity (TCHC), Sheffield (Project code CA11024). Partial support was also provided by the EPSRC Frontier Grant (MultiSim project code EP/K03877X/1).

References

Arundel, P., Ahmed, S.F., Allgrove, J., Bishop, N.J., Burren, C.P., Jacobs, B., Mughal, M. Z., Offiah, A.C., Shaw, N.J., 2012. British paediatric and adolescent bone group's position statement on vitamin D deficiency. BMJ 345, e8182.

Bayraktar, H.H., Morgan, E.F., Niebur, G.L., Morris, G.E., Wong, E.K., Keaveny, T.M., 2004. Comparison of the elastic and yield properties of human femoral trabecular and cortical bone tissue. J. Biomech. 37, 27–35.
Bennett, L.B., Pierce, M.C., 2010. Bone health and development. In: Jenny, C. (Ed.), Child Abuse and Neglect: Diagnosis, Treatment, and Evidence. Elsevier Inc., St. Louis, Missouri.
Berteau, J.-P., Pithioux, M., Baron, C., Gineyts, E., Follet, H., Lasaygues, P., Chabrand, P., 2012. Characterization of the difference in fracture mechanics between children and adult cortical bone. Comput. Methods Biomech. Biomed. Eng. 15, 281–282.
Cardadeiro, G., Baptista, F., Ornelas, R., Janz, F.K., Sardinha, B.L., 2012. Sex specific association of physical activity on proximal femur BMD in 9 to 10 year old children. PLoS One 7, e50657.
Cohen, M.C., Offiah, A., Sprigg, A., Al-Adnani, M., 2013. Vitamin D deficiency and sudden unexpected death in infancy and childhood: A cohort study. Pediatr. Dev. Pathol. 16, 292–300.
Cristofolini, L., Schileo, E., Juszczyk, M., Taddei, F., Martelli, S., Viceconti, M., 2010. Mechanical testing of bones: the positive synergy of finite-element models and in vitro experiments. Philos. Trans. R. Soc. A. Math., Phys. Eng. Sci. 368, 2725–2763.
Currey, D.J., Brear, K., Zioupos, P., 1996. The effects of ageing and changes in mineral content in degrading the toughness of human femora. J. Biomech. 29, 257–260.
Currey, D.J., Butler, G., 1975. The mechanical properties of bone tissue in children. J. Bone Jt. Surg. 57, 810–814.
Currey, D.J., Pond, M.C., 1989. Mechanical properties of very young bone in the axis deer and humans. J. Zool. (Lond.) 218, 59–67.
Fassier, A., Gaucherand, P., Kohler, R., 2013. Fractures in children younger than 18 months. Orthop. Traumatol.: Surg. Res. 99, S160–S170.
Grassi, L., Schileo, E., Taddei, F., Zani, L., Juszczyk, M., Cristofolini, L., Viceconti, M., 2012. Accuracy of finite element predictions in sideways load configurations for the proximal human femur. J. Biomech. 45, 394–399.
Hirsch, C., Evans, F.G., 1965. Studies on some physical properties of infant compact bone. Acta Orthop. Scand. XXXV, 300–313.
Kemper, C.G.H., 2000. Skeletal development during childhood and adolescence and the effects of physical activity. Pediatr. Exerc. Sci. 12, 198–216.
Kontulainen, S.A., Hughes, J.M., Macdonald, H.M., Johnston, J.D., 2007. The biomechanical basis of bone strength development during growth. Med. Sport Sci. 51, 13–32.
McCalden, W.R., Mcgeough, A.J., Court-Brown, M.C., 1997. Age related changes in the compressive strength of cancellous bone. J. Bone Jt. Surg. A 79, 421–427.
McKay, H., Smith, E., 2008. Winning the battle against childhood physical inactivity: The key to bone strength? J. Bone Miner. Res. 23, 980–985.
Morgan, E.F., Bayraktar, H.H., Keaveny, T.M., 2003. Trabecular bone modulus-density relationships depend on anatomic site. J. Biomech. 36, 897–904.
Mosekilde, L., Mosekilde, L., Danielsen, C.C., 1987. Biomechanical competence of vertebral trabecular bone in realtion to ash density and age in normal individuals. Bone 8, 79–85.
Ohman, C., Baleani, M., Pani, C., Taddei, F., Alberghini, M., Viceconti, M., Manfrini, M., 2011. Compressive behaviour of child and adult cortical bone. Bone 49, 769–776.
Pierce, M.C., Bertocci, G.E., Vogeley, E., Moreland, M.S., 2004. Evaluating long bone fractures in children: A biomechanical approach with illustrative cases. Child Abuse Negl. 28, 505–524.
Scheuer, L., Black, M.S., Craig, C., Christie, A., 2000. Developmental Juvenile Osteology. Elsevier, London, UK.
Schileo, E., Dall'ara, E., Taddei, F., Malandrino, A., Schotkamp, T., Baleani, M., Viceconti, M., 2008a. An accurate estimation of bone density improves the accuracy of subject-specific finite element models. J. Biomech. 41, 2483–2491.
Schileo, E., Taddei, F., Cristofolini, L., Viceconti, M., 2008b. Subject-specific finite element models implementing a maximum principal strain criterion are able to estimate failure risk and fracture location on human femurs tested in vitro. J. Biomech. 41, 356–367.
Schileo, E., Taddei, F., Malandrino, A., Cristofolini, L., Viceconti, M., 2007. Subject-specific finite element models can accurately predict strain levels in long bones. J. Biomech. 40, 2982–2989.
Schoenau, E., Fricke, O., 2008. Mechanical influences on bone development in children. Eur. J. Endocrinol. 159 (Suppl 1), S27–S31.
Specker, L.B., 2006. Influence of rapid growth on skeletal adaptation to exercise. J. Musculoskelet. Neuronal Interact. 6, 147–153.
Taddei, F., Pancanti, A., Viceconti, M., 2004. An improved method for the automatic mapping of computed tomography numbers onto finite element models. Med. Eng. Phys. 26, 61–69.
Taddei, F., Schileo, E., Helgason, B., Cristofolini, L., Viceconti, M., 2007. The material mapping strategy influences the accuracy of CT-based finite element models of bones: an evaluation against experimental measurements. Med. Eng. Phys. 29, 973–979.
Taddei, F., Viceconti, M., Manfrini, M., Toni, A., 2003. Mechanical strength of a femoral reconstruction in paediatric oncology: a finite element study. Proc. Inst. Mech. Eng., Part H: J. Eng. Med. 217, 111–119.
Vinz, H., 1969. Die festigkeitsmechanischen Grundlagen der typischen Frakturformen des Kindesalters. Zentralblatt Chir. 94, 1509–1515.
Vinz, H., 1970. Die Anderung der Festikeitseigenschaften des kompakten Knochengewebes im Laufe der Altersentwicklung. Gegenbaurs Morphol. Jahrb. 115, 257–272.
Vinz, H., 1972. Die Festigheit der reinen Knochensubstanz. Naherungsverfahren zur Bestimmung der auf den hohlraumfreien Querschnitt bezogenen Festigkeit von Knochengewebe. Gegenbaurs Morphol. Jahrb. 117, 453–460.
Wallace, J.I., Kwaczala, T.A., Judex, S., Demes, B., Carlson, J.K., 2013. Physical activity engendering loads from diverse directions augments the growing skeleton. J. Musculoskelet. Neuronal Interact. 13, 283–288.
Weaver, K.J., 1966. The microscopic hardness of bone. J. Bone Jt. Surg. A 48, 273–288.
Wu, G., Siegler, S., Allard, P., Kirtley, C., Leardini, A., Rosenbaum, D., Whittle, M., D'lima, D.D., Cristofolini, L., Witte, H., Schmid, O., Stokes, I., Standardization and Terminology Committee of the International Society of Biomechanics, 2002. ISB recommendation on definitions of joint coordinate system of various joints for the reporting of human joint motion - Part I: ankle, hip, and spine. International society of biomechanics. J. Biomech. 35, 543–548.
Yamada, T., 1970. Strength of Biological Materials. In: Evans, F.G. (Ed.), 1970. Williams and Wilkins Co., Baltimore, MD.
Zannoni, C., Mantovani, R., Viceconti, M., 1998. Material properties assignment to finite element models of bone structure: A new method. Med. Eng. Phys. 20, 735–740.